Phylogenetic Measures of the Core Microbiome

Sharon Anne Bewick[1]*, Benjamin Thomas Camper[1]

[1]Department of Biological Sciences, Clemson University, Clemson, South Carolina 29631, USA

*sbewick@clemson.edu

Abstract

Background: A useful concept in microbial ecology is the 'core microbiome.' Typically, core microbiomes are defined as the microbial taxa, genes, or functions shared by a threshold number of microbiome samples from a particular type of habitat (e.g., a particular type of host or a particular type of environment/ecosystem). In defining the core microbiome, the goal is to capture the portion of the microbial community that is conserved across samples from the focal habitat. Recently, there has been growing interest in developing methods to better characterize core microbiomes. As a result, numerous occurrence- and abundance-based measures have been defined. However, few have included phylogeny-aware metrics for analyzing core microbiomes. Results: In this paper, we develop the concept of the 'core community phylogeny' – a phylogeny where branches are selected based on their presence in multiple samples from a single type of habitat. We then use the core community phylogeny to define phylogenetic metrics describing the diversity of core microbiomes from a single type of habitat, the turnover between core microbiomes from two different types of habitats, and the shared diversity across core microbiomes from two or more different types of habitats. As compared to non-phylogenetic metrics, our phylogenetic metrics show greater consistency across taxonomic rank and/or

phylogenetic level, as well as less sensitivity to strain variation across microbiome samples. Thus, our metrics address key challenges in the interpretation of core microbiomes. Conclusions: We provide a phylogenetic framework for characterizing and comparing core microbiomes. Importantly, the methods that we propose allow seamless integration of microbiome properties across taxonomic rank and/or phylogenetic level. Ultimately, this will provide both a more consistent picture of the core microbiome, as well as novel biological insight into the conserved components of microbial communities.

Introduction

Core microbiomes have become increasingly important as a dimension for studying and characterizing sets of microbial communities.[1,2] Broadly speaking, a core microbiome is the group of microbial taxa, genes, or functions shared by a large number of microbiome samples from a specific type of habitat. Often, the habitat is defined based on a host species[3–5] (e.g., the core microbiome of the human gut[6]), or a specific type of ecosystem (e.g., the core microbiome of a particular soil type[7]). However, much broader[8] (e.g., the core microbiome of ruminant guts[9]) and much narrower (e.g., the core microbiome of a particular host population[10] or host genotype[11]) habitat classes can be used as well. Because core microbial taxa are commonly, if not always, associated with a specific habitat, they are thought to be important for identifying microbial persistence requirements within the habitat, predicting ecosystem function[12–15] or, in the case of host-associated microbiomes, understanding symbiotic relationships that may be important to host performance.[16–19] By contrast, it is generally assumed that microbial taxa occurring only sporadically in a given habitat are more likely to be transients or other community members that do not contribute substantially to host or ecosystem function.

While the concept of a core microbiome is both simple and appealing, how to best define the core microbiome of any given habitat remains unclear.[1,2] In general, three different core criteria have been proposed[1] based on 1) the occupancy (i.e., incidence rate, frequency of occurrence) of microbial taxa across samples, 2) the abundance of microbial taxa in individual samples or across a set of samples, or 3) a combination of occupancy and abundance criteria.[20,21] Within these three strategies, however, there are a wide range of parameters that can influence interpretation. One obvious example is the threshold occupancy or abundance that a microbial taxon must achieve to be considered part of the core. In some cases, microbial taxa are included in the core if they are found in at least two samples from a given habitat.[1] In other cases, much higher core thresholds have been used, such as requiring that a microbial taxon be present in half or even all of the samples from a particular habitat. Some studies even present analyses across a range of core thresholds so that results can be interpreted in context.[22,23]

Beyond the occupancy and abundance thresholds, another decision that can influence identification of core microbial taxa is the taxonomic rank or phylogenetic level at which the core microbiome is defined. Studies exist spanning a wide range of taxonomic ranks and phylogenetic levels from phyla to genera and from 97% operational taxonomic units (OTUs) to amplicon sequence variants (ASVs).[1] Not surprisingly, examining the core microbiome at different taxonomic and/or phylogenetic scales often results in different conclusions. Higher taxonomic ranks like phyla and order tend to be more conserved across samples, resulting in a larger proportion of microbial taxa being identified as part of the core. However, ecology and function tend to be less conserved at these higher taxonomic ranks[24,25], making the core

microbiome less useful for informing host or ecosystem ecology. By contrast, at very low taxonomic ranks, it is unclear whether variation between microbial taxa has significant ecological or functional consequences. ASVs, for example, may only differ by one base pair in the portion of the marker gene used for sequencing.[26] However, in microbial taxa with multiple copies of the 16S rRNA marker gene, individual gene copies can vary intragenomically by >1%.[27,28] Thus, ASVs may be much more diverse than the populations or functions that they are being used to represent.[29] This can impact the core microbiome in one of two ways. First, if multiple closely related ASVs are present in a threshold number of samples, they may all be counted individually as part of the core, inflating core diversity. Second, if individual samples each contain unique but closely related ASVs, none of the ASVs may occur in sufficient samples to be included in the core, reducing core diversity. Perhaps because of the challenges associated with defining core microbiomes at very high and very low taxonomic and/or phylogenetic scales, most analyses of core microbiomes have used intermediate scales, for example 97% operational taxonomic units (OTUs) or genera.[1]

The importance of taxonomic and/or phylogenetic scale, and the apparent variation in study outcomes as a function of the taxonomic/phylogenetic scale considered are not unique to analysis of core microbiomes.[1] Indeed, these same challenges occur in more general types of ecological analyses of both microbial and macrobial systems, for example, calculation of α- and β-diversity in and between ecological communities. This has led to the development of different phylogeny-aware metrics including Faith's phylogenetic diversity[30] (PD), Rao's quadratic entropy[31] and phylogenetic entropy[32] for α-diversity, and UniFrac distances[33] for β-diversity. Phylogeny-aware metrics are advantageous because they integrate information across taxonomic ranks based on

92 the branch lengths in a phylogenetic tree. This removes the need to select an arbitrary taxonomic
93 rank or phylogenetic level for any particular ecological analysis. Further, because some
94 phylogenetic properties can serve as indicators of both functional diversity[34] and evolutionary
95 potential[35] (i.e., capacity to evolve in response to a perturbation, for example environmental
96 change[36–38]), phylogeny-aware metrics often provide more informative comparisons[39] of
97 properties like diversity than do analyses at any single taxonomic or phylogenetic scale.
98
99 Despite the many benefits of phylogeny-aware ecological analyses, few phylogeny-aware
100 methods for characterizing the core microbiome exist. Several recent papers have begun to
101 account for phylogeny when characterizing core microbiomes[40–42], for instance by defining core
102 taxa based on a series of clustering thresholds.[43] Nevertheless, there remains a lack metrics that
103 smoothly integrate phylogenetic information across taxonomic and phylogenetic scales. In this
104 paper, we develop a framework for analyzing core microbiomes using phylogenetic methods. To
105 do this, we first develop the concept of a 'core community phylogeny' - a phylogeny where
106 branches are defined based on being present in multiple samples from a single type of host or
107 environment. We then use this phylogeny to examine common measures of core communities,
108 including Venn diagrams, as well as metrics of within- and between-habitat diversity.
109
110 **Core Community Phylogenies**
111
112 All phylogeny-aware metrics of ecological communities, for example Faith's phylogenetic
113 diversity (PD) and UniFrac distance, are based on an underlying phylogenetic tree comprising
114 taxa present in the community. Logically, the analogous phylogenetic tree for core microbiomes

115 should comprise all microbial taxa that are conserved across microbiomes from a particular type
116 of habitat. However, for core microbiomes, there are two possible ways of defining such a tree: a
117 'tip-based' approach, and a 'branch-based' approach.
118
119 ***Tip-based phylogeny:*** One way to build a core community phylogeny is to first identify core
120 microbial taxa based on their relative abundance and/or occupancy across a threshold number of
121 microbiome samples from a particular type of habitat. Once these microbial taxa have been
122 identified, a phylogenetic tree can be reconstructed based on the sequences (or other traits) of the
123 conserved taxa. Notably, conserved microbial taxa can be identified at any pre-selected
124 taxonomic rank (e.g., phyla, genera, 97% OTUs, ASVs, etc.) provided that a phylogenetic tree
125 can be built connecting the various microbial lineages. The tip-based phylogeny is useful in that
126 it incorporates phylogeny while still identifying extant microbial taxa that comprise the core.
127 However, because the tip-based phylogeny identifies core taxa without reference to their
128 phylogenetic relationships, it does not capitalize fully on phylogenetic information.
129 Consequently, metrics calculated using the tip-based phylogeny are more susceptible to variation
130 across taxonomic rank and/or phylogenetic level as compared to metrics calculated using the
131 branch-based approach that we discuss next (see 'Examples' and 'Discussion' for more details).
132
133 ***Branch-based phylogeny:*** An alternative way to build a core community phylogeny is to first
134 build a phylogeny of all microbial taxa present in a set of microbiome samples from a particular
135 type of habitat. This phylogenetic tree can then be examined, branch-by-branch, to determine
136 which branches satisfy core criteria based occupancy and/or abundance thresholds (i.e., which
137 branches occur in sufficient numbers of samples or have sufficient abundance associated with

138 them). Branches that satisfy the core criteria can then be retained, while branches that do not can
139 be discarded. Note that, at least for a rooted tree, this results in discarding shallow branches
140 connected to deeper branches that have also been discarded, such that the remaining phylogeny
141 is fully connected (but see below for issues that arise with unrooted trees). Like the tip-based
142 phylogeny, the branch-based phylogeny can have leaf nodes at any taxonomic rank. However,
143 because the branch-based phylogeny integrates information on shared microbial lineages across
144 all depths of the phylogeny both for defining the core and calculating core metrics, there is less
145 reason to use high taxonomic levels (see 'Examples' below). Thus, we recommend ASVs as the
146 default choice.
147
148 Importantly, the tip-based phylogeny and the branch-based phylogeny for a given system will not
149 always be identical. Whereas the branch-based phylogeny will always have all of the branches
150 present in the tip-based phylogeny, the tip-based phylogeny will often be missing some of the
151 branches present in the branch-based phylogeny (see Figure 1). More specifically, the tip-based
152 phylogeny will be missing branches whenever a set of microbiome samples share closely related,
153 but not identical, taxa. In this case, none of the shallow branches will be considered core for
154 either the tip-based or the branch-based phylogeny. However, the deeper branches from which
155 all of the related tips are derived may be present on the threshold number of samples and thus
156 may be retained in the branch-based phylogeny. By contrast, these branches will be discarded in
157 the tip-based phylogeny, since definition of core is solely based on shared leaf nodes. This
158 fundamental difference is what makes the branch-based approach less sensitive to variations in
159 the precise taxonomic scale considered, at least when making relative comparisons between two
160 or more core communities (see 'Examples' below).

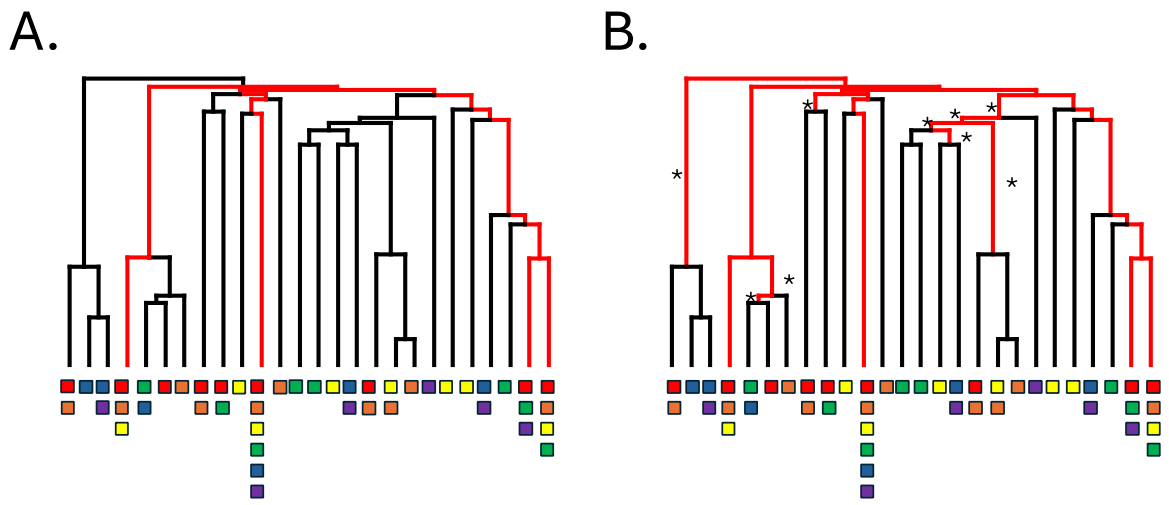

Figure 1. Examples of a tip-based phylogeny (A) and a branch-based phylogeny (B) for the same microbial phylogeny. Branches of the microbial phylogeny that are not part of the core community phylogeny are shown in black, while branches that are part of the core community phylogeny are shown in red. For this example dataset, there are 6 samples (red, orange, yellow, green, blue, and purple squares) and we use an occupancy threshold of 0.5 as our core criterion. Thus being part of the core requires being present in 3 samples. Colored boxes at the end of each terminal branch indicate the samples that a particular microbial taxon is present on. Stars are used to mark branches that are included in the branch-based phylogeny but not in the tip-based phylogeny.

Figure 1 shows the construction of both a tip-based phylogeny (A) and a branch-based phylogeny (B) from the same set of microbiome samples and based on an occurrence threshold of 0.5 (i.e., a taxon must occur in at least 50% of samples to be considered part of the core). In Figure 1, the non-core branches of the microbial phylogeny are shown in black, while the core branches are shown in red. Notice that there are differences between the tip-based phylogeny and the branch-based phylogeny (see starred branches). In particular, the branch-based phylogeny includes additional internal branches that are missing from the tip-based phylogeny. This occurs because some clades are represented in 50% of samples, and thus are part of the branch-based

core microbiome, even though the individual taxa within the clades are not present in 50% of samples.

***Rooted versus Unrooted Trees*:** An important consideration in defining the core community phylogeny is whether to assume that the root node is the most recent common ancestor (MRCA) of all taxa in the sample. The root node should only be used as the MRCA when a rooted tree is provided. Otherwise, the root node is arbitrary, and there is no reason to believe that the root node is any more basal than the other nodes in the tree. Fortunately, microbial phylogenies generated using pipelines like Qiime2[44] usually have the option for rooting trees (although this is typically done through midpoint rooting, which involves multiple assumptions). Similar to UniFrac, we strongly encourage using a rooted tree and forcing the root node to be the MRCA. This is particularly true for branch-based core community phylogenies. The reason is as follows: using the branch-based approach, branches are counted based on their inclusion in individual phylogenies from each sample. When a root node is defined, these individual sample phylogenies necessarily include the root. In absence of a root, however, individual sample phylogenies only span the taxa present in each sample (core or otherwise). Consequently, basal branches may not be counted if entire clades are differentially distributed across subsets of samples. When this happens, distinct clades are not necessarily connected in the phylogeny that emerges. To remedy this, we connect the final core community phylogeny based on the MRCAs for all of the distinct clades. This, however, does not guarantee that branches will not be lost in the process. For tip-based phylogenies, the choice to use an unrooted tree is less problematic because the branches of the core community phylogeny are selected based on the occupancy of

203 microbial taxa (tip nodes), not on the occupancy of the branches themselves. Even for tip-based
204 trees, however, we recommend using a rooted tree and assuming that the root node is the MRCA.
205
206 ***Criteria for Inclusion:*** Another important consideration in defining the core community
207 phylogeny is the criterion used to determine whether a taxon or branch is part of the core. The
208 simplest option is to use an occupancy threshold. Core taxa could, for example be selected based
209 on being present in 50%, 90% or 100% of samples from a particular type of habitat.
210 Alternatively, various relative abundance thresholds could be used, either by themselves or in
211 combination with an occupancy threshold. Core taxa could, for instance, be selected based on
212 attaining a mean or minimum relative abundance across all samples or based on reaching a
213 maximum relative abundance in at least one sample. Whereas occupancy thresholds imply a
214 degree of conservation across samples, abundance thresholds indicate numerical dominance
215 (with the caveat that measured dominance may be different from true dominance due to biases in
216 extraction, PCR, etc.). When used in combination, occupancy and abundance thresholds allow
217 the core to be selected based on both conservation and numerical dominance.
218
219 While occupancy and abundance thresholds are the simplest forms of core criteria, several other
220 definitions have been developed as well. Recently, for instance, Shade and Stopnisek[20] have
221 pioneered a method that identifies core taxa based on being both strongly conserved within a
222 habitat and contributing to variation across that habitat. Fundamentally different from the
223 threshold approach, this more nuanced method can, in some cases, be more powerful than simple
224 occupancy and abundance thresholds. Importantly, identification of a core community phylogeny
225 does not depend on the use of any particular core criterion. Rather, core community phylogenies

226 can, at least theoretically, be defined based on any criterion that can be applied to individual
227 taxonomic units. For the tip-based tree, this means applying the chosen criterion when selecting
228 core taxa. For the branch-based tree, this means applying the chosen criterion on a branch-by-
229 branch basis.
230
231 **Phylogenetic Metrics for Core Microbiomes**
232 Once a core community phylogeny has been constructed, it can be used to perform phylogenetic
233 analyses of microbiome samples from different types of habitats. Here we consider several
234 common analysis methods, including Venn diagrams, a core microbiome equivalent of Faith's
235 phylogenetic diversity (α-diversity), and a core microbiome equivalent of UniFrac distance (β-
236 diversity).
237
238 ***Venn Diagrams*:** Venn diagrams are one of the most common methods for visualizing core
239 microbiomes across habitats. Non-phylogenetic Venn diagrams show counts of the core
240 microbial taxa shared by different combinations of habitat types. This can be extended to a
241 phylogenetic framework by replacing counts of shared microbial taxa with shared phylogenetic
242 branch lengths. Briefly, the core community phylogenies from different habitat types can be
243 compared, branch-by-branch, to determine which branches appear in which habitat
244 combinations. The total lengths of these shared branch segments can then be calculated and
245 reported either as an absolute value or as percentages of the total branch length spanning the core
246 community phylogenies of all habitats in the analysis.
247

248 ***Core Faith's Phylogenetic Diversity* (PD):** The phylogenetic equivalent to richness (a count of
249 microbial taxa present in a community), Faith's PD is the sum of the branch lengths of all
250 branches spanning the taxa present in a particular microbiome sample or ecological community.
251 This definition can easily be extended to core microbiomes by summing the branch lengths of all
252 branches in the core community phylogeny. Doing so gives a measure of how much
253 phylogenetic diversity is conserved across microbiome samples from a particular type of habitat.
254
255 ***Core UniFrac Distances*:** The phylogenetic equivalent to Jaccard's index[45] (the fraction of
256 unique microbial taxa between two communities), the UniFrac distance[33,46] between two
257 communities is the sum of the branch lengths that are unique to each microbiome sample or
258 ecological community divided by the sum of the branch lengths of all branches spanning taxa
259 present in both microbiome samples or ecological communities. Again, this definition can be
260 extended to core microbiomes by dividing the branch lengths unique to each core community
261 phylogeny by the total branch lengths of the two core community phylogenies combined. Doing
262 so gives a measure of how phylogenetically distinct the core microbiomes are from two different
263 types of habitats.
264
265 **Examples**
266 Additional file 1: Simple Example System (see Figures S1.1 and S1.2) outlines the calculation of
267 Venn diagrams, core Faith's PD, and core UniFrac distances using a set of highly simplified core
268 community phylogenies. In this additional file, we show differences between tip- and branch-
269 based approaches, and outline calculations with both rooted and unrooted trees. Throughout the

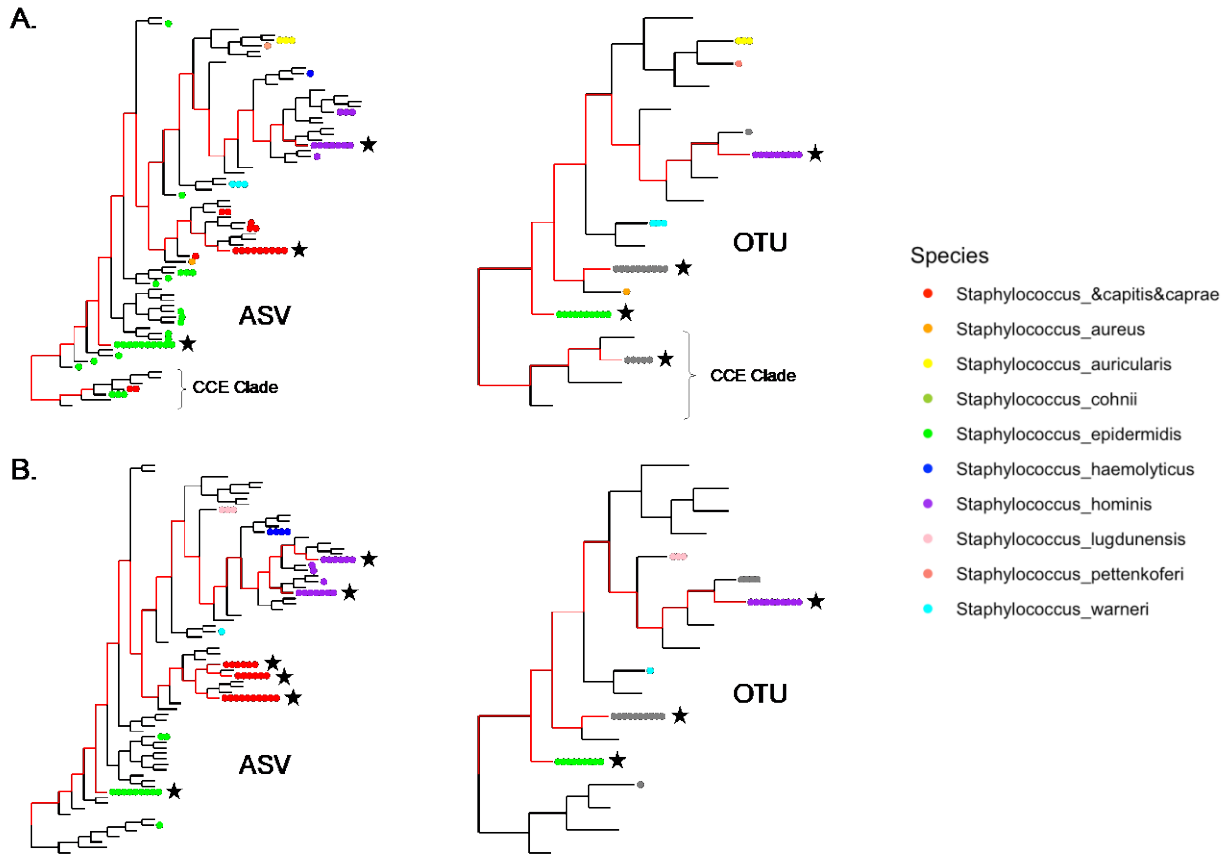

Figure 2 *Staphylococcus* phylogenies for 10 skin microbiome samples from two individuals - Individual One (A) and Individual Two (B) - using ASVs (left) and OTUs (right). Circles at the end of each terminal branch indicate the number of samples that contained the corresponding ASV or OTU. These circles are colored based on assigned species, with grey being used when multiple species are contained within the same OTU. Black stars indicate taxa that would be part of each individual's core microbiome based on a non-phylogenetic approach using an occupancy threshold of 50%. Red lines indicate branches that are part of each individual's core microbiome based on a branch-based phylogenetic approach using the same occupancy threshold of 50%. Because the terminal branches on these trees are extremely short, trees are visualized using a square root transformation. This transformation was not used in calculating core microbiota.

remainder of the main text, we apply our methods to more realistic systems using rooted trees. First, we consider the *Staphylococcus* component of the human skin microbiota based on a dataset from Joglekar et al.[47] For this analysis, we use the branch-based phylogeny combined with a simple occupancy threshold of 50% (i.e., a taxon/branch must be present in 50% of

287 samples to be considered part of the core, for alternate core criteria see Additional file 1:
288 Additional *Staphylococcus* Analyses, Figures S2.1-S2.3). Figure 2 shows *Staphylococcus* taxa
289 present in skin samples from two different people, first based on amplicon sequence variants
290 (ASVs) and then based on operational taxonomic units (OTUs, see 'Methods' for more details).
291 Core taxa that would be identified based on a non-phylogenetic approach are identified with
292 black stars. Core branches identified based on our phylogenetic approach are colored red. The
293 *Staphylococcus* microbiota on these two individuals demonstrate the challenges faced by non-
294 phylogenetic definitions of the core microbiome: whereas Individual One (Fig. 2A) has a lower
295 core *Staphylococcus* diversity based on ASVs (3 versus 6), Individual Two (Fig. 2B) has a lower
296 core *Staphylococcus* diversity based on OTUs (3 versus 4). Two separate phenomena explain this
297 diversity reversal. First, on Individual One, there are two ASVs from the CCE Clade (see Figure
298 2A) that do not, independently, reach an occupancy threshold of 50% and thus fail to contribute
299 to core ASV richness. When these ASVs are pooled into a single OTU, however, the OTU is
300 present in 50% of samples and thus is counted as part of the core. This leads to an increase in
301 diversity at the OTU scale and reflects the fact that strain variation across samples from
302 Individual One obscured the relatively high occupancy of closely related *Staphylococcus* in the
303 CCE clade. Second, on Individual Two, three closely related *S. capitis/caprae* strains and two
304 closely related *S. hominis* strains separately contribute to core ASV richness. These ASVs are,
305 however, pooled and counted as single core taxa at the OTU scale. This leads to a reduction in
306 OTU diversity and reflects the fact that most of the ASV diversity on Individual Two was a
307 result of shallow strain variation within the *S. capitis/caprae* and *S. hominis* clades. Unlike non-
308 phylogenetic measures of core *Staphylococcus* diversity, phylogenetic measures do not vary as
309 much across phylogenetic levels. Rather, phylogenetic measures suggest that the core microbiota

310 of the first person is more diverse at both the ASV (0.169 vs. 0.113) and OTU (0.180 vs. 0.105)
311 scales. The explanation is simple: the relatively fewer core ASVs on Individual One span a wider
312 phylogenetic breadth than the numerous but closely related ASVs on Individual Two (See
313 Additional file 1: Additional *Staphylococcus* Analyses for further comparisons across individuals
314 from the Joglekar et al.[47] study). Rank reversals in diversity estimates as a function of
315 phylogenetic scale can be problematic because they can make it difficult to interpret differences
316 between treatment groups. Using a non-phylogenetic approach, for instance, it might be difficult
317 to assess whether or not core *Staphylococcus* diversity increases resistance to pathogens like
318 methicillin-resistant *S. aureus* (MRSA).[48,49] This is because the people considered to have high
319 versus low core *Staphylococcus* diversity changes depending on the phylogenetic scale
320 considered. By contrast, the stability of our phylogenetic metrics across all phylogenetic scales
321 makes them more amenable to exploring relationships between core *Staphylococcus* diversity
322 and disease resistance.
323
324 Figure 3 shows a comparison of the core *Staphylococcus* microbiota across skin habitats from the
325 same Jonglekar et al.[47] study, along with turnover (β-diversity) in core *Staphylococcus*
326 composition among habitats. Again, differences in the phylogenetic and non-phylogenetic
327 approaches are apparent. Based on the non-phylogenetic Jaccard distance, for instance, the core
328 *Staphylococcus* microbiota of the nares is highly distinct from the core *Staphylococcus*
329 microbiota of all other skin habitats. This distinction, however, is much less obvious when using
330 a tip-based UniFrac distance and non-existent when using a branch-based UniFrac distance.
331 Indeed, the branch-based UniFrac distance suggests that the core *Staphylococcus* microbiota of

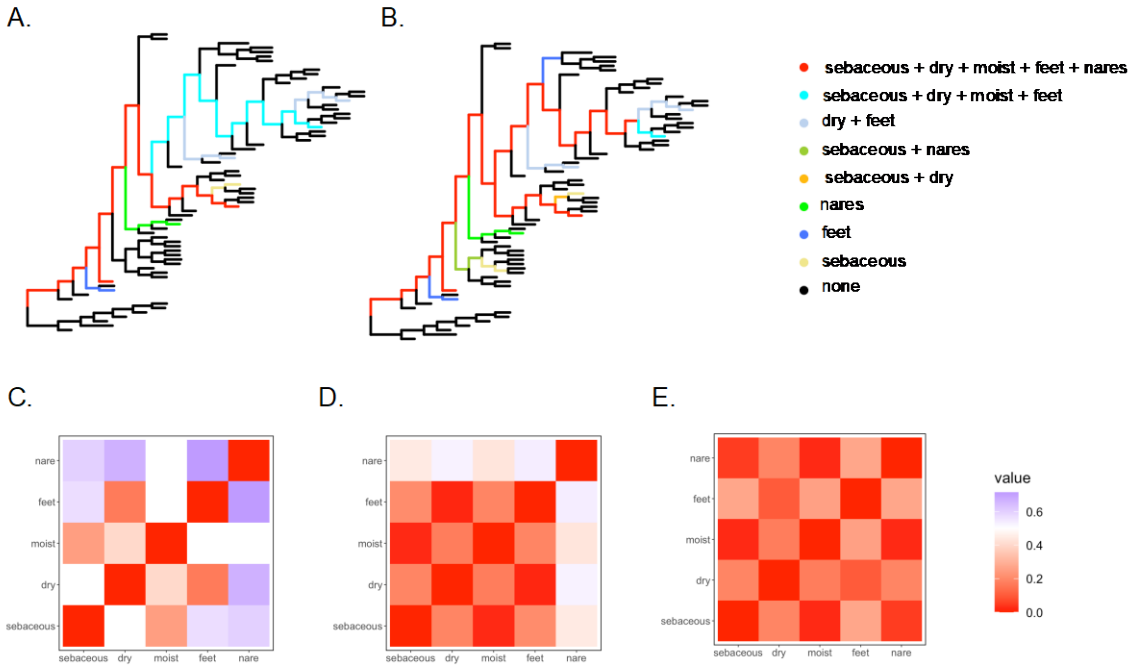

Figure 3 (A) Tip-based and (B) branch-based *Staphylococcus* phylogenies showing the shared and unique core community phylogenies, along with Jaccard distances (C), tip-based UniFrac distances (D) and branch-based UniFrac distances (E) among skin habitats. All panels in this figure used a 50% occupancy threshold as the core criterion. Because the terminal branches on these trees are extremely short, trees are visualized using a square root transformation. This transformation was not used in calculating core microbiota.

the nares is actually quite similar to the core *Staphylococcus* microbiota of both moist and sebaceous sites. Inspection of the phylogenetic trees for the tip- and branch-based approaches explains these differences. In particular, the nares are missing an *S. hominis* ASV found in the core *Staphylococcus* microbiota all other skin habitats. The nares are not, however, entirely lacking *S. hominis* ASVs. Rather, the nares are colonized by a range of other *S. hominis* ASVs, though none individually reaches the threshold for core inclusion. Nevertheless, because multiple *S. hominis* ASVs are present in nares samples, the branch-based approach counts most of the diversity associated with the *S. hominis* clade towards the core microbiota of both the nares and the other four habitat classes (sebaceous, moist, dry, feet). It is only the shallow tip branches that

do not contribute towards the core microbiota of the nares. By contrast, for the tip-based and non-phylogenetic approaches, the missing *S. hominis* ASV drives significant turnover between the nares and all other sites.

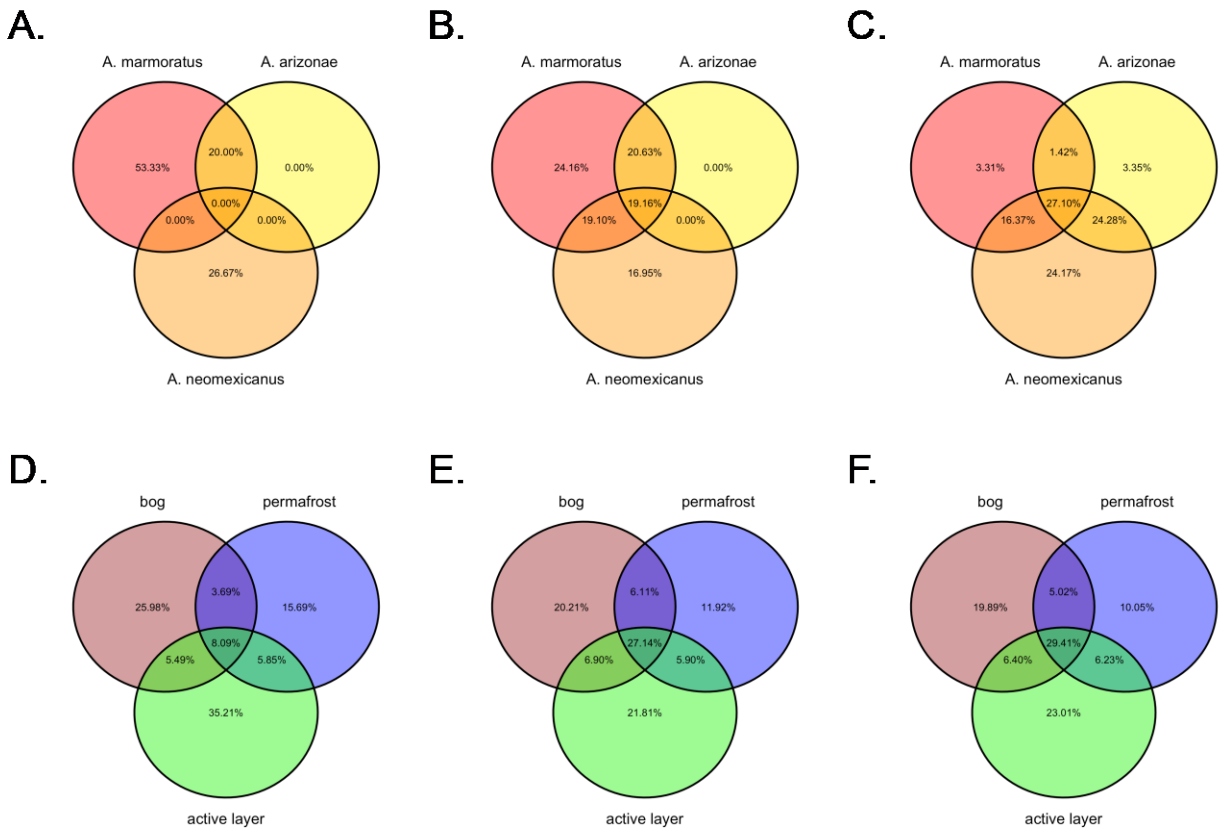

Figure 4. Venn diagrams for lizard gut (A-C) and soil (D-F) microbiota showing the percentage of the total ASV counts shared by the core microbiota from each lizard species or soil type (A, D) and the phylogenetic branch length shared by the core microbiota from each lizard species or soil type using either tip-based (B, E) or branch-based (C, F) phylogenies. In all Venn diagrams, lizard populations and soil types colored are as follows: *Aspidoscelis arizonae* (yellow), *A. neomexicanus* (orange), *A. marmoratus* (red), bog soil (brown), permafrost soil (blue) and seasonally thawed active layer soil (green).

365 Having demonstrated the benefits of our phylogenetic approach on a relatively simple and low
366 diversity *Staphylococcus* system, we next turn our attention to two additional datasets – one host-
367 associated and the other environmental – both of which contain significant diversity and multiple
368 bacterial phyla. Specifically, we consider the gut microbiota of three different whiptail lizard
369 (*Aspidoscelis*) species and the soil microbiota of three different soil types (see Materials and
370 Methods). Figure 4 shows standard Venn diagrams based on ASV counts (A, D) along with our
371 new phylogenetic Venn diagrams for tip-based (B, E) and branch-based (C, F) trees. For all
372 Venn diagrams, we define the core based on a 50% occupancy threshold (for alternate core
373 criteria, see Additional file 1: Additional Venn Diagrams). As compared to our phylogenetic
374 Venn diagrams, non-phylogenetic Venn diagrams (A, D) show the lowest percentage of system
375 diversity in the compartments representing the intersections of (A) gut microbiota of all three
376 lizard species (0%) and (D) microbiota of all three soil types (8.02%). Non-phylogenetic Venn
377 diagrams also show the highest percentage of system diversity in (A) the three compartments
378 unique to single lizard species (80.00%) and (D) the three compartments unique to individual
379 soil types (76.88%). This is not surprising. Using a non-phylogenetic approach, microbial taxa
380 from different host species/environments must be identical to be counted in intersection
381 compartments. This biases against finding shared microbial diversity, particularly when using
382 ASVs, because microbial lineages with small differences in 16S rRNA gene sequences (e.g., one
383 base pair substitutions) are deemed unique. By contrast, with a phylogenetic approach, even if
384 different host populations/environments have slightly different ASVs, this only contributes a
385 small amount of diversity to the unique compartments of the Venn diagram. Meanwhile, the
386 majority of the diversity is allotted to intersection compartments because the ASVs from the
387 different host populations/environments share most of their phylogenetic history. Comparing

388 branch-based and tip-based phylogenetic approaches, branch-based phylogenies show a higher
389 percentage of system diversity in the compartments representing intersection across (B, C) all
390 three lizard species (27.10% vs. 19.16%) and (E, F) soil types (29.41% vs. 27.14%). This reflects
391 the inclusion of additional, deep internal branches in branch-based phylogenies that are dropped
392 from tip-based phylogenies (see Figure 1). These basal branches are more likely to be conserved
393 across different host species/environments (i.e., phyla are more likely to be shared than ASVs),
394 inflating diversity in shared compartments of the Venn diagram (see Additional file 1: Additional
395 Venn Diagrams Figures S3.1-S3.4 for several additional datasets, including lizard skin and lake
396 water).
397
398 Figure 5 (A-C) shows core richness, and tip- and branch-based core Faith's PD as a function of
399 taxonomic rank for lizard gut microbiota based on an occupancy threshold (A), an occupancy
400 and abundance threshold (B) and the Shade and Stopnisek core criterion (C). For the sake of
401 comparison across metrics and taxonomic rank, we have plotted core diversity of two lizard
402 species (yellow: *A. arizonae*; red: *A. marmoratus*) relative to the third lizard species (*A.*
403 *neomexicanus*; see Materials and Methods). Figure 5 (E-G) shows similar plots for soil
404 microbiota, this time agglomerating taxa based on cophenetic distance, rather than taxonomy.
405 Again, for the sake of comparison, we have plotted core diversity of bog (brown) and active
406 layer (green) soils relative to permafrost soils. Figure 5 (D, H) shows the range of values
407 obtained for core richness and tip- and branch-based Faith's PD across all taxonomic ranks/tip
408 agglomerations considered. In most cases, phylogenetic measures of lizard gut and soil
409 microbiota show less variation across taxonomic rank/tip agglomeration as compared to non-
410 phylogenetic measures. Using an occupancy threshold of 50%, for instance, the richness of the

411 core gut microbiota of *A. marmoratus* (red) is anywhere from 0.64 (microbial species) to 2.75
412 (microbial ASV) times as diverse as the core gut microbiota of *A. neomexicanus*. By contrast, for
413 the same occupancy threshold, the branch-based core Faith's PD suggests a much narrower range
414 from 0.52 (microbial ASV) to 0.62 (microbial order). Likewise, using the Shade and Stopnisek
415 criterion, the richness of the core microbiota of active layer soil is anywhere from 0.92
416 (agglomeration: h = 0.15) to 1.5 (ASV) times as diverse as the core microbiota of permafrost
417 soil. Meanwhile, for the same Shade and Stopnisek criterion, the branch-based core Faith's PD
418 exhibit a much narrower range from 1.19 (agglomeration: h = 0.15) to 1.22 (ASV). Not all
419 differences in metric stability across taxonomic rank/tip agglomeration are as dramatic. Still, the
420 branch-based core Faith's PD typically shows the least variation across taxonomic ranks/tip
421 agglomeration, while the tip-based core Faith's PD shows the second least variation, and
422 richness shows the most variation. Nevertheless, there are deviations to this general trend,
423 particularly for the Shade and Stopnisek criterion (see Additional File 1: Additional α- and β-
424 diversity Analyses Figures S4.1 and S4.2 for several additional datasets, including lizard skin
425 and lake water).
426

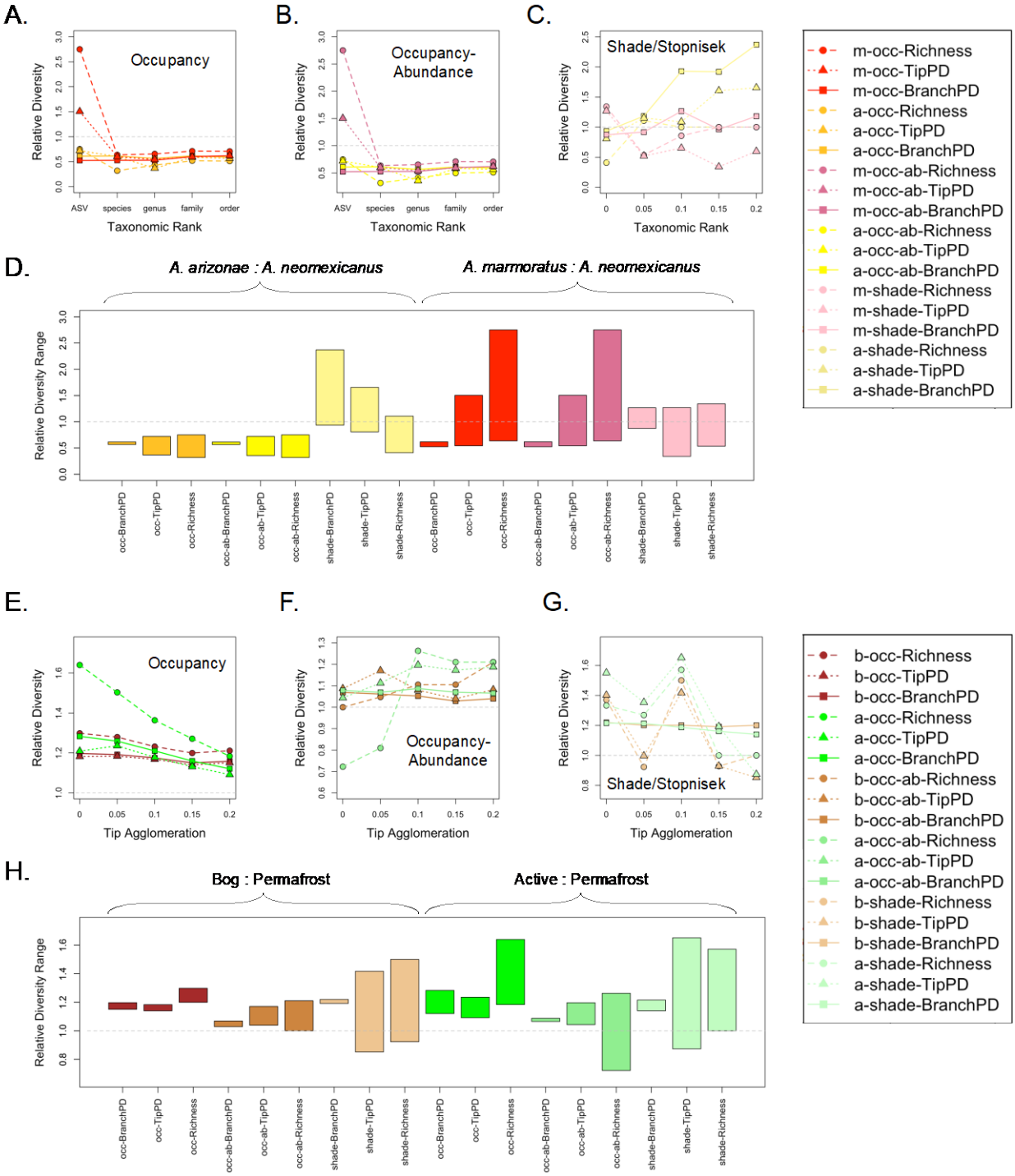
A.
Occupancy
Relative Diversity
ASV
species
genus
family
order
Taxonomic Rank
B.
Occupancy-Abundance
Relative Diversity
Taxonomic Rank
C.
Shade/Stopnisek
Relative Diversity
Taxonomic Rank
m-occ-Richness
m-occ-TipPD
m-occ-BranchPD
a-occ-Richness
a-occ-TipPD
a-occ-BranchPD
m-occ-ab-Richness
m-occ-ab-TipPD
m-occ-ab-BranchPD
a-occ-ab-Richness
a-occ-ab-TipPD
a-occ-ab-BranchPD
m-shade-Richness
m-shade-TipPD
m-shade-BranchPD
a-shade-Richness
a-shade-TipPD
a-shade-BranchPD
D.
A. arizonae : A. neomexicanus
A. marmoratus : A. neomexicanus
Relative Diversity Range
occ-BranchPD
occ-TipPD
occ-Richness
occ-ab-BranchPD
occ-ab-TipPD
occ-ab-Richness
shade-BranchPD
shade-TipPD
shade-Richness
E.
Occupancy
Relative Diversity
Tip Agglomeration
F.
Occupancy-Abundance
Relative Diversity
Tip Agglomeration
G.
Shade/Stopnisek
Relative Diversity
Tip Agglomeration
b-occ-Richness
b-occ-TipPD
b-occ-BranchPD
a-occ-Richness
a-occ-TipPD
a-occ-BranchPD
b-occ-ab-Richness
b-occ-ab-TipPD
b-occ-ab-BranchPD
a-occ-ab-Richness
a-occ-ab-TipPD
a-occ-ab-BranchPD
b-shade-Richness
b-shade-TipPD
b-shade-BranchPD
a-shade-Richness
a-shade-TipPD
a-shade-BranchPD
H.
Bog : Permafrost
Active : Permafrost
Relative Diversity Range
occ-BranchPD
occ-TipPD
occ-Richness
occ-ab-BranchPD
occ-ab-TipPD
occ-ab-Richness
shade-BranchPD
shade-TipPD
shade-Richness

Figure 5. Comparison of alpha diversity across taxonomic ranks (A-C) and degrees of tip agglomeration (E-G, see Materials and Methods) for the branch-based Core Faith's PD (solid, squares), the tip-based Core Faith's PD (dotted, triangles), and richness (dashed, circles) assuming the following core criteria: (A,E) an occupancy threshold of 50% (gold, red, dark brown, bright green), (B,F) an occupancy threshold of 50% and a mean abundance threshold of 0.1% (yellow, dark pink, medium brown, medium green), (C,G) the Shade and Stopnisek method (light yellow, light pink, light brown, light green). In (A-C), we show the core diversity of *Aspidoscelis arizonae* (gold, yellow, pale yellow) and *A. marmoratus* (red,dark pink, light pink) gut microbiota relative to the core diversity of *A. neomexicanus* gut microbiota. In (E-G) we show the core diversity of bog (dark, intermediate and light brown) and active layer (bright, intermediate and light green) soil microbiota relative to the core diversity of permafrost soil microbiota. Bar graphs (D,H) showing minimum and maximum values of alpha diversity across taxonomic rank for *A. arizonae* (gold, yellow, light yellow) and *A. marmoratus* (red, dark pink, light pink) relative to *A. neomexicanus*, and across tip agglomeration for bog soil (dark, intermediate and light brown) and active layer soil (bright, intermediate and light green) relative to permafrost soil. Diversity metrics are indicated as follows: 'BranchPD' is the branch-based phylogeny approach, 'TipPD' is the tip-based phylogeny approach, and 'Richness' is a count of taxa for each taxonomic rank. Core criteria are indicated as follows: 'occ' is the 50% occupancy threshold, 'occ-ab' is the 50% occupancy and 0.1% abundance threshold, and 'shade' is the Shade and Stopnisek method.

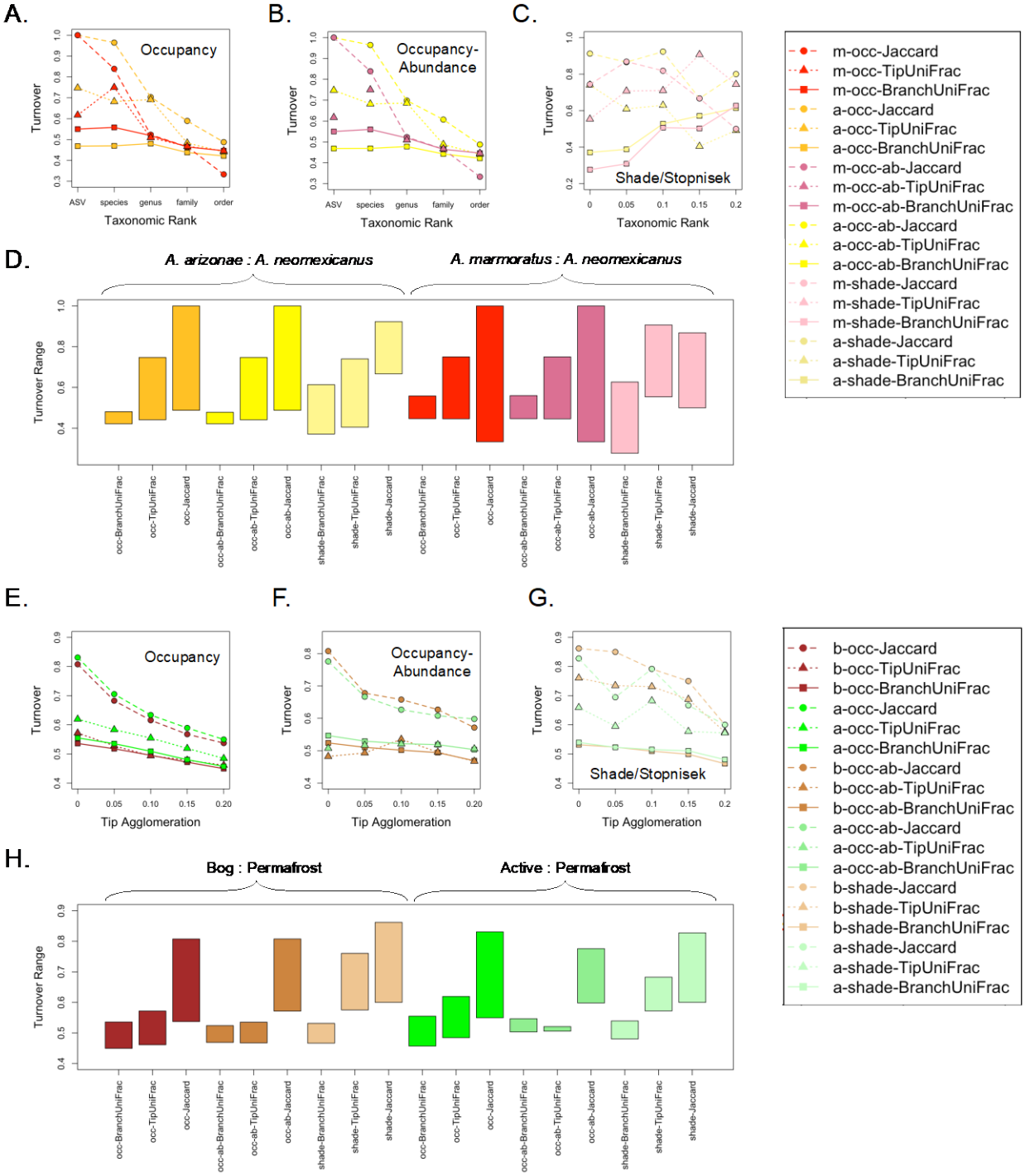
A.
Occupancy
Turnover
Taxonomic Rank
ASV
species
genus
family
order
B.
Occupancy-Abundance
C.
Shade/Stopnisek
m-occ-Jaccard
m-occ-TipUniFrac
m-occ-BranchUniFrac
a-occ-Jaccard
a-occ-TipUniFrac
a-occ-BranchUniFrac
m-occ-ab-Jaccard
m-occ-ab-TipUniFrac
m-occ-ab-BranchUniFrac
a-occ-ab-Jaccard
a-occ-ab-TipUniFrac
a-occ-ab-BranchUniFrac
m-shade-Jaccard
m-shade-TipUniFrac
m-shade-BranchUniFrac
a-shade-Jaccard
a-shade-TipUniFrac
a-shade-BranchUniFrac
D.
A. arizonae : A. neomexicanus
A. marmoratus : A. neomexicanus
Turnover Range
occ-BranchUniFrac
occ-TipUniFrac
occ-Jaccard
occ-ab-BranchUniFrac
occ-ab-TipUniFrac
occ-ab-Jaccard
shade-BranchUniFrac
shade-TipUniFrac
shade-Jaccard
E.
Occupancy
Tip Agglomeration
F.
Occupancy-Abundance
G.
Shade/Stopnisek
b-occ-Jaccard
b-occ-TipUniFrac
b-occ-BranchUniFrac
a-occ-Jaccard
a-occ-TipUniFrac
a-occ-BranchUniFrac
b-occ-ab-Jaccard
b-occ-ab-TipUniFrac
b-occ-ab-BranchUniFrac
a-occ-ab-Jaccard
a-occ-ab-TipUniFrac
a-occ-ab-BranchUniFrac
b-shade-Jaccard
b-shade-TipUniFrac
b-shade-BranchUniFrac
a-shade-Jaccard
a-shade-TipUniFrac
a-shade-BranchUniFrac
H.
Bog : Permafrost
Active : Permafrost

457 **Figure 6.** Comparison of beta diversity across taxonomic ranks (A-C) and degrees of tip
458 agglomeration (E-G, see Materials and Methods) for the branch-based Core UniFrac distance
459 (solid, squares), the tip-based Core UniFrac distance (dotted, triangles), and Jaccard distance
460 (dashed, circles) assuming the following core criteria: (A,E) an occupancy threshold of 50%
461 (gold, red, dark brown, bright green), (B,F) an occupancy threshold of 50% and a mean
462 abundance threshold of 0.1% (yellow, dark pink, medium brown, medium green), (C,G) the
463 Shade and Stopnisek method (light yellow, light pink, light brown, light green). In panels (A-C),
464 we show turnover of *A. arizonae* (gold, yellow, light yellow) and *A. marmoratus* (red, dark pink,
465 light pink) gut microbiota relative to *A. neomexicanus* gut microbiota. In panels (E-G) we show
466 turnover of bog (dark, intermediate and light brown) and active layer (bright, intermediate and
467 light green) soil microbiota relative to permafrost soil microbiota. Bar graphs (D,H) showing
468 minimum and maximum values of beta diversity (turnover or distance) across taxonomic rank
469 for *A. arizonae* (gold, yellow, light yellow) and *A. marmoratus* (red, dark pink and light pink)
470 relative to *A. neomexicanus* and across tip agglomeration for bog soil (dark, intermediate and
471 light brown) and active layer soil (bright, intermediate and light green) relative to permafrost
472 soil. Diversity metrics are as follows: where 'BranchUniFrac' is the branch-based phylogeny
473 approach, 'TipUniFrac' is the tip-based phylogeny approach, and 'Jaccard' is a count of taxa for
474 each taxonomic rank/tip agglomeration. Core criteria are indicated as follows: 'occ' is the 50%
475 occupancy threshold, 'occ-ab' is the 50% occupancy and 0.1% abundance threshold, and 'shade'
476 is the Shade and Stopnisek method.
477

478

479 Figure 6 (A-C) shows the Jaccard, tip- and branch-based UniFrac distances between core gut
480 microbiota of *A. neomexicanus* and both *A. arizonae* (yellow) and *A. marmoratus* (red) based on
481 an occupancy threshold (A), an occupancy and abundance threshold (B) and the Shade and
482 Stopnisek core criteria (C). Figure 6 (E-G) shows similar plots for soil microbiota, this time
483 agglomerating taxa based on cophenetic distance, rather than taxonomy. Figure 6 (D, E) shows
484 the range of values obtained for Jaccard, tip- and branch-based UniFrac distances across all
485 taxonomic ranks/tip agglomerations considered. Broadly speaking, the branch-based approach
486 gives the smallest distances, as well as the least variation across taxonomic rank/tip
487 agglomeration. Meanwhile the tip-based approach gives intermediate distances and intermediate
488 variation and the non-phylogenetic approach (i.e., Jaccard distance) gives the largest distances

489 and the most variation (see Additional file 1: Additional α- and β-diversity Analyses Figures
490 S4.1 and S4.2 for several additional datasets, including lizard skin and lake water).
491
492 **The holobiont R package**
493 To facilitate the use of our new phylogenetic measures of core microbiomes, we developed a
494 new R package, holobiont, that includes functions for identifying the core community
495 phylogeny in any microbiome, drawing phylogenetic Venn diagrams, calculating the core Faith's
496 PD for a set of communities, and calculating the core UniFrac distance between two sets of
497 communities. Briefly, the coreEdges function takes a phyloseq object[50] and the core criterion
498 and identifies the branches of the core community phylogeny. The coreTree function takes the
499 same information and colors the branches of the core community phylogeny red, while leaving
500 the remaining branches of the community tree black. The corePhyloVenn function takes a
501 phyloseq object, a vector defining the habitat class for each microbiome sample, and the core
502 criterion and draws a phylogenetic Venn diagram of either branch lengths or percentages of
503 branch lengths shared by the core community phylogenies of different combinations of habitat
504 classes. The coreVennTree function takes the same input as the corePhyloVenn function and
505 colors the branches of the phylogenetic tree based on the combination of habitat class core
506 community phylogenies that they belong to. The coreFaithsPD function takes a phyloseq object
507 and the core criterion and calculates the core Faith's PD. Finally, the coreUniFrac function takes
508 a phyloseq object and a vector specifying which samples belong to which habitat class
509 (maximum 2) and calculates the UniFrac distance between the core community phylogenies. In
510 addition to the phylogenetic functions, the holobiont package also provides corresponding non-
511 phylogenetic functions, including coreTaxa, coreVenn, coreRichness and coreJaccard.

Additional details outlining the methods and use of our R package can be found on the CRAN website at https://cran.r-project.org/web/packages/holobiont/index.html. A brief discussion of our modified Shade and Stopnisek algorithm can be found in Additional file 1: Shade and Stopnisek Algorithm.

Discussion

In this paper, we propose a framework for performing phylogeny-aware analyses of core microbiomes. More specifically, we develop the concept of a core community phylogeny - a phylogeny based on the microbial lineages that are core to a specific habitat class. We then propose two different methods for selecting this tree - a tip-based approach and a branch-based approach. For the tip-based approach, core membership is decided based on occupancy and/or abundance of the leaf (tip) nodes. This is akin to the standard, non-phylogenetic method for defining a core microbiome. However, once members of the core microbiome have been identified, a phylogenetic tree is constructed. This allows for calculation of phylogeny-aware metrics that leverage the relatedness of the leaf nodes to determine overall properties (e.g., diversity) of the core microbiome. For the branch-based approach, core membership is decided independently for each branch of the phylogenetic tree. Therefore, in the branch-based approach, phylogeny informs not only the calculation of metrics but also, the identification of the core microbiome itself. The downside of the branch-based approach, however, is that the 'core microbiome' often includes internal nodes while excluding their associated leaf nodes. Thus, metrics calculated using the branch-based approach are not necessarily based on a set of extant taxa. Rather, they are based on a set of complete and partial microbial lineages (see, for example, Figure 2A, where branches leading to the CCE clade are included in the branch-based core

535 phylogeny, even though all terminal branches from this clade are excluded). Still, because the
536 branch-based approach uses phylogenetic information to both define the core microbiome and to
537 calculate core metrics, we suggest using the branch-based approach except when there is a strong
538 desire to identify specific microbial taxa within the core (e.g., to select for culturing
539 experiments).
540
541 As compared to existing metrics, the primary advantage of our phylogenetic metrics is that they
542 seamlessly integrate core microbiome properties (i.e., richness, turnover, shared taxa) across
543 taxonomic scales/phylogenetic levels. Thus, our phylogenetic metrics are more likely to provide
544 biologically relevant information. This is especially true when non-phylogenetic metrics are
545 calculated at taxonomic ranks that fail to capture meaningful biological variation.[51] If, for
546 example, the chosen taxonomic rank is too low, substantial biological variation may be identified
547 that has no functional or ecological consequences. Alternatively, if the chosen taxonomic rank is
548 too high, large amounts of meaningful biological variation may be pooled into the same
549 taxonomic unit. Depending on the system, the type of variation considered and the metric
550 calculated, it can be difficult to *a priori* determine (or even *a posteriori* assess) which taxonomic
551 ranks are more or less likely to be biologically informative. Further, in certain instances multiple
552 taxonomic ranks exhibit substantial meaningful biological variation. In this case, a non-
553 phylogenetic metric at any single taxonomic rank - even a well-chosen taxonomic rank - cannot
554 fully capture the underlying signal. Phylogenetic metrics circumvent these challenges by
555 summarizing the full spectrum of biological variation across all taxonomic ranks, with variation
556 at lower taxonomic ranks weighted less than variation at higher taxonomic ranks.
557

558 Another benefit of our branch-based approach (but not our tip-based approach) is that it
559 overcomes challenges associated with defining the core microbiome in the face of high levels of
560 strain variation. This is common in certain microbiome systems, including many host-associated
561 microbiomes. The pervasive human skin isolate, *Staphylococcus epidermidis*, for example,
562 evolves on individual humans over time,[52,53] resulting in strain level variation across the human
563 population. Another common human skin isolate, *Cutibacterium acnes*, exhibits even more
564 dramatic strain-level variation, showing differences in sequences across pores from a single
565 human individual.[54] Indeed, in-depth profiling of the human microbiome has shown that there
566 are numerous personalized microbial taxa that are found on only one or several individuals.[53,55]
567 Depending on the taxonomic rank at which the core microbiome is defined and the degree to
568 which any single microbial strain is shared among individual hosts, natural strain-level variation
569 can cause broadly shared microbial clades to be obscured from the non-phylogenetic core
570 microbiome. By contrast, if we apply our branch-based approach to these same scenarios, only
571 the terminal branches of the tree are omitted. Meanwhile, the more basal branches of the clades
572 are retained because they are shared across all strains. We see this in our simple *Staphylococcus*
573 example in Figure 2A, where the basal branches of the CCE clade are retained in the branch-
574 based approach despite none of the extant ASVs from this clade reaching the non-phylogenetic
575 threshold for core inclusion.
576
577 Because our phylogenetic metrics summarize microbiome measures across taxonomic
578 rank/phylogenetic level and because the definition of the core microbiome - at least when using
579 the branch-based approach - is less sensitive to strain-level variation, our phylogenetic metrics
580 tend to be more consistent than comparable non-phylogenetic metrics when calculated at

581 different taxonomic and/or phylogenetic scales. This is true both in a relative (i.e., comparison
582 between microbiome samples) and an absolute sense. To see why phylogenetic metrics are more
583 consistent, consider a habitat with hundreds of closely related core microbial strains within a
584 single phylum. Using a non-phylogenetic approach, this system will have a very high ASV α-
585 diversity (i.e., ASV richness), but a very low phylum α-diversity (i.e., phylum richness). By
586 contrast, using our phylogenetic approach, α-diversity (i.e., Faith's PD) will be low regardless of
587 whether the leaf nodes are defined at the ASV- or phylum-level. This is because, even when the
588 leaf nodes are ASVs, all of the different ASV strains contribute very short branch lengths.
589 Consequently, they do not substantially inflate α-diversity beyond the diversity of the single
590 phylum. The greater consistency of our phylogenetic metrics across taxonomic ranks means that
591 it is less important to choose the correct taxonomic rank, and that it is rarely disadvantageous to
592 use ASVs. This addresses one of the challenges that has been raised about interpreting core
593 microbiomes when outcomes are variable across taxonomic rank or phylogenetic level.[1]
594
595 While our phylogenetic metrics typically yield lower variation across taxonomic rank and/or
596 phylogenetic level, this is not always the case, particularly when using the Shade and Stopnisek
597 criterion. Exactly why phylogenetic metrics are more variable when combined with the Shade
598 and Stopnisek criterion is unclear. This may have to do with the emphasis that the Shade and
599 Stopnisek method places on microbiome variation rather than microbiome conservation.
600 Alternatively, it may be related to the stopping criterion used to delineate the Shade and
601 Stopnisek core. Notably, changing the stopping criterion can impact the relative variation of
602 phylogenetic and non-phylogenetic measures as a function of taxonomic rank (see Additional
603 File 1: Shade and Stopnisek Algorithm Figure S5.1). While our phylogenetic metrics may not

604 provide as much stabilization for the Shade and Stopnisek method, they still appear to perform as
605 well or better in most cases. In our calculations of core α- and β-diversity for lizard guts and
606 soils, for instance, our branch-based phylogenetic metric was more stable in 7/8 scenarios
607 (though the differences were marginal in 2/8 scenarios), and only less stable in 1/8 scenarios (see
608 Figures 5 and 6). Thus, even for the Shade and Stopnisek method, the branch-based approach
609 appears to be advantageous.
610
611 The primary goal of this paper is to introduce a framework for phylogenetic analysis of core
612 microbiomes. For this reason, we have focused on the concepts required to define a core
613 community phylogeny and have outlined the application of a core community phylogeny to three
614 types of microbiome analyses - Venn diagrams, α-diversity (Faith's PD), and β-diversity
615 (UniFrac). Our broad approach, however, is not limited to these particular types of analyses.
616 Indeed, additional analyses could be developed within the same framework. A straightforward
617 example would be to use UniFrac distances between core microbiomes to project into ordination
618 space (e.g., Principal Coordinate Analysis or Nonmetric Multidimensional Scaling). This would
619 provide phylogenetically informed visualization of the relatedness of different core microbiomes.
620
621 While initially developed for microbiome analysis, beyond microbiomes, our community
622 phylogenetics approach and associated R package may ultimately have wide application to
623 macrobial systems as well. Currently, very few macrobial studies attempt to identify core
624 communities (but see Murdock et al.[56]). This is likely because, at least historically, macrobial
625 systems have not been studied with many replicates. Indeed, even when replicate macrobial
626 communities are characterized, the effort required to identify all taxa in a single community

627 means that replicate numbers are low. This makes it difficult to identify a core community.
628 Further, in species poor macrobial systems where characterization of replicate communities is
629 possible, the core community concept is not as necessary or useful because the systems are
630 simple enough to analyze in their entirety. As sequencing techniques improve, however, and
631 more and more macrobial systems are characterized in a manner similar to microbiomes (e.g.,
632 through the use of eDNA[57,58]), it seems likely that core communities will emerge as a common
633 form of analysis for species rich macrobial systems (e.g., tropical rainforests or litter insects) as
634 well. There is no reason why our proposed framework cannot be applied to macrobial
635 communities. In fact, our framework can be applied to any system including prokaryotic and
636 eukaryotic communities, host-associated and free-living communities, and microbial (virus,
637 bacteria, fungi, etc.) and macrobial communities. It can also be applied to systems characterized
638 through a wide variety of methods, even including non-sequencing techniques. The only
639 requirements for our approach are tables of presences/absences of different taxa across different
640 communities, along with a phylogenetic tree comprising all taxa present across all communities.
641 Thus, occupancy data can be based on sequencing but can also be based on any other form of
642 observation, including transect or plot surveys. Likewise, phylogenies can be constructed using
643 sequence data, including sequencing of any kind (single marker genes, combinations of marker
644 genes, whole genomes), but can also be generated based on morphology or other traits
645 commonly used to build trees. While any phylogeny can be used for our phylogenetic analysis of
646 core communities, the validity of the analysis will depend on the accuracy of the phylogeny;
647 thus, care should be taken to select the most appropriate approach to tree building given the data
648 available. For 16S rRNA gene sequencing, Qiime2 provides guidance and pipelines for both
649 alignment-based and fragment-insertion methods of tree reconstruction.[44] Likewise, for shotgun

650 metagenomics sequencing, the Genome Taxonomy Database tookit (GTDB-Tk)[59,60] provides
651 different options for both *de novo* tree reconstruction and placement of genomes into a reference
652 tree.
653
654 The identification and characterization of core microbiomes has become a hallmark of
655 microbiome analysis. However, to date, most analyses of core microbiomes have focused on
656 taxonomy at specified taxonomic ranks. By contrast, phylogeny-aware metrics for characterizing
657 core microbiomes are largely lacking. Phylogeny-aware metrics have the benefit of integrating
658 information across taxonomic ranks. This can be particularly helpful when analysis at different
659 taxonomic ranks yields different outcomes - a common problem in ecology and evolution[61–65]
660 including the study of core microbiomes.[1] Our phylogenetic framework overcomes this
661 challenge. Indeed, even when our analysis is performed at different taxonomic ranks, it typically
662 yields more consistent results than non-phylogenetic methods. With the development of our new
663 framework and associated R package, we provide a mechanism to bring phylogeny-aware
664 community analyses to the study of core microbiomes. Ultimately, this will allow for novel
665 insight into the conserved components of microbial communities both within and between
666 different types of habitats.
667
668 **Methods**
669 ***Datasets***
670 Skin *Staphylococcus* microbiota: We downloaded the ps_staph_ASV_filter_final.rds file from
671 https://github.com/skinmicrobiome/Joglekar_Staphylococcus_2023/tree/main/phyloseq_object.
672 We then loaded this file into R and used it to write out a FASTA file of representative sequences.

673 From the FASTA file, we used the align-to-tree-mafft-fasttree pipeline in Qiime2 to construct
674 a phylogenetic tree for all *Staphylococcus* ASVs based on their 16S rRNA sequences. The
675 FASTA file of representative sequences is available on our GitHub page. Next, we rarified
676 samples to a read depth of 500 using the rarefy_even_depth function from the phyloseq
677 package (version 1.50.0).[50] For our analysis of individuals, we randomly selected 10 skin
678 samples from all 9 individuals with 10+ skin samples available (recognizing that different body
679 sites were used for different people). We then compared core microbiota across individuals based
680 on ASVs and OTUs. For the latter, we agglomerated closely related taxa using the tip_glom
681 function from the phyloseq package (h = 0.5). For our analysis of skin habitats, we randomly
682 selected 20 skin samples from all 5 habitats with 20+ skin samples available (sebaceous, moist,
683 dry, feet, nares). We performed all analyses of the *Staphylococcus* dataset using an unscaled
684 phylogenetic tree. However, because many of the terminal branches were short, for the sake of
685 visualization, we plotted the *Staphylococcus* phylogenies using a square-root transformation.
686
687 Lizard gut microbiota: We sampled the microbiota from several whiptail lizard species (genus
688 *Aspidoscelis*, family *Teiidae*) at two locations (see Camper et al.[66] for more site details) within
689 Sevilleta National Wildlife Refuge. Each location represents a site of syntopy between hybrid *A.*
690 *neomexicanus* and a progenitor species, *A. marmoratus* (♀; a heterogenous grassland-mesquite
691 shrubland site: 34.397882°N, 106.867637°W, WGS84) and *A. arizonae* (♂, recently split from
692 *A. inornatus*[67]; a grassland site with sparse cholla cacti: 34.331178°N, 106.636717°W, WGS84).
693 Following taxonomic guidelines by Tucker et al.[68] and Walker et al.,[69] we refer to *Aspidoscelis*
694 spp. using the masculine epithet. We captured lizards using a rapidly deployable drift fence
695 trapping array lined with box funnel traps, further outlined in Camper et al.,[66] and by hand or

696 lizard noose when possible. Upon capture, we sampled the gut (=cloacal) and skin microbiota
697 (for analysis of the skin dataset, see Additional file 1) of each species following a swabbing
698 protocol in Camper et al.[22] We sampled each location until we captured at least 15 female lizards
699 of each whiptail species. All samples were sent to ZymoBIOMICS Targeted Sequencing Service
700 for Microbiota Analysis (Zymo Research) using 16S rRNA gene sequencing. Additional details
701 are available from https://www.zymoresearch.com/pages/16s-its-amplicon-sequencing and
702 Camper et al.[22] FASTQ files for lizard microbiomes, as well as environmental and sequencing
703 controls, are available at (these will be uploaded to NCBI upon publication).
704
705 We used FASTA files of representative sequences, supplied to us by ZymioBIOMICS Targeted
706 Sequencing Service (available on our GitHub page: https://github.com/bewicklab/CoreTrees/), to
707 create phylogenetic trees, as described above. We then combined these trees with the .biom files,
708 also supplied to us by the ZymoBIOMICS Targeted Sequencing Service (also available
709 at: https://github.com/bewicklab/CoreTrees/) for all downstream analysis. Details on the Zymo
710 pipeline can be found in our previous description of the dataset.[22] Prior to analysis, we removed
711 16S rRNA gene sequences that could not be identified as Bacteria or Archaea based on the
712 proprietary Zymo database. Additionally, we removed all samples with a read depth lower than
713 10,000 reads. Finally, we rarefied all samples to the read depth of the lowest sample. [49]
714
715 Soil dataset: We downloaded dataset 1036 from redbiom
716 (https://qiita.ucsd.edu/study/description/1036).[70] We then used the feature-table.qza file and
717 the all.seqs.fa files from the 130932 folder. From the FASTA file, we constructed a phylogeny,
718 again using the same Qiime2 pipeline that was used for the *Staphylococcus* dataset. We then read

719 the resulting feature table and phylogeny into R for analysis. For α-diversity, we rarefied
720 samples to the size of the sample with the lowest read depth. For β-diversity, we rarefied samples
721 to 5000 reads because of the computational time required by the tip_glom function for larger
722 datasets (see below).
723
724 Lake dataset: We downloaded dataset 1041 from redbiom
725 (https://qiita.ucsd.edu/study/description/1041). We then used the feature-table.qza file and the
726 reference-hit.seqs.fa files from the 131527 folder. From the FASTA file, we constructed a
727 phylogeny, again using the same Qiime2 pipeline that was used for the *Staphylococcus* dataset.
728 We then read the resulting feature table and phylogeny into R for analysis. For both α-and β-
729 diversity, we rarefied samples to the size of the sample with the lowest read depth. Analysis of
730 the lake dataset can be found in Additional file 1.
731
732 ***Dataset Analysis***
733 Core Trees: We used the coreEdges function from our holobiont package to identify branches
734 of the *Staphylococcus* phylogeny that were core to each individual. We then visualized the trees
735 using a modification of the plot_phylo function from the phyloseq package (included in the
736 code on our Github page). We used the coreVennTree function from our holobiont package to
737 identify and visualize branches of the *Staphylococcus* phylogeny that were shared by the core
738 microbiota of different skin habitats. For all figures in the main text, we used an occupancy
739 threshold of 0.5 as our core criterion.
740

741 Venn Diagrams: We used the coreVenn and corePhyloVenn functions from our holobiont
742 package to create non-phylogenetic and phylogenetic Venn Diagrams respectively. In all cases,
743 we reported percentages of the total branch length and used rooted phylogenies. All Venn
744 diagrams in the main text were calculated based on rooted trees for ASVs using an occupancy
745 threshold of 0.5 as our core criterion. Additional core criteria are included in Additional file 1:
746 Additional Venn Diagrams.
747
748 α-diversity: We used the coreRichness and coreFaithsPD functions from our holobiont
749 package to calculate non-phylogenetic and phylogenetic α-diversity respectively. To compare
750 across taxonomic ranks, we took the original ASV .biom file supplied by Zymo or .qza file
751 downloaded from redbiom to generate an ASV phyloseq object.[50] We then used the tax_glom
752 and tip_glom functions from the phyloseq package to generate OTU tables and phylogenies for
753 the lizard and soil/lake datasets respectively. For tax_glom, we considered taxonomic ranks from
754 species ('Rank7') through to order ('Rank4'). For tip_glom we considered cophenetic distances
755 from h = 0.05 to h = 0.2. This allowed us to calculate Faith's PD at different taxonomic
756 ranks/levels of tip agglomeration, as well as related non-phylogenetic richness. All Faith's PD
757 and richness calculations were performed on rooted trees using the following core criteria: (1) an
758 occupancy threshold of 0.5, (2) an occupancy threshold of 0.5 and a mean relative abundance
759 threshold of 0.1% and (3) a modified Shade and Stopnisek method (see Additional File 1: Shade
760 and Stopnisek Algorithm).
761
762 β-diversity: We used the coreJaccard and coreUniFrac functions from our holobiont package
763 to calculate non-phylogenetic and phylogenetic β-diversity respectively. Comparisons across

taxonomic ranks/tip agglomeration were performed as described for Faith's PD. Again, all UniFrac and Jaccard calculations were performed on rooted trees using the following core criteria: (1) an occupancy threshold of 0.5, (2) an occupancy threshold of 0.5 and a mean relative abundance threshold of 0.1% and (3) a modified Shade and Stopnisek method.

All analyses were performed using the R programming language[71] (version 4.2.1) available on our Github page at: https://github.com/bewicklab/CoreTrees

Declarations

Ethics approval and consent to participate

All research was approved by Clemson University under IACUC protocol numbers #2020-015 and #2021-047. We completed this work under the Sevilleta National Wildlife Refuge Special Use Permit #SEV_Bewick_Camper_2022_59 and the New Mexico Department of Game and Fish permit authorization #3772.

Consent for publication

not applicable

Funding

This study was funded by NSF awards #2105604 and #2025541, a Clemson University Support for Early Exploration and Development (CUSEED) Grant, and the Clemson University Creative Inquiry (CI) Program.

Availability of data and materials

All data and code (BIOM files, metadata files, and all R code) necessary for the analyses presented in this manuscript are available at https://github.com/bewicklab/CoreTrees unless otherwise noted in the main text. All data (BIOM and metadata files) are further included as a zipped file as Additional file 2. The holobiont R package is publicly available through CRAN, available at https://cran.r-project.org/web/packages/holobiont/index.html. We have uploaded all raw sequence data (lizard microbiota and controls) to the National Center for Biotechnology Information's SRA database (https://dataview.ncbi.nlm.nih.gov/object/PRJNA1188019?reviewer=9hrl0g7nl4fmdqf8icgjglbes2), and this information will be made publicly available upon acceptance.

Competing interests

The authors declare that they have no competing interests.

Authors' contributions

BTC and SAB conceived the idea and wrote the first draft of the manuscript. BTC performed all related fieldwork. SAB developed the code and data analysis. All authors contributed substantially to the content of the manuscript.

Acknowledgements

We thank Thomas Dempster, August Spencer, Eva Purcell, Riley Manuel, Drew Kanes and Zachary Laughlin for their field assistance in New Mexico as well as Lily Margeson, Simon Dunn, Georgianna Bellinger, Henry Egloff, Kaila Hodges, Camryn Lachica, and Savannah Utz for their assistance assembling drift fence trapping arrays.

References

1. Neu AT, Allen EE, Roy K. Defining and quantifying the core microbiome: Challenges and prospects. *Proceedings of the National Academy Sciences*. 2021;118(51):1-10. doi:10.1073/pnas.2104429118/-/DCSupplemental
2. Custer GF, Gans M, van Diepen LTA, Dini-Andreote F, Buerkle CA. Comparative Analysis of Core Microbiome Assignments: Implications for Ecological Synthesis. *mSystems*. 2023;8(1):1-14. doi:10.1128/msystems.01066-22
3. Huse SM, Ye Y, Zhou Y, Fodor AA. A core human microbiome as viewed through 16S rRNA sequence clusters. *PLoS One*. 2012;7(6):1-12. doi:10.1371/journal.pone.0034242
4. Zaura E, Keijser BJ, Huse SM, Crielaard W. Defining the healthy "core microbiome" of oral microbial communities. *BMC Microbiol*. 2009;9(259):1-12. doi:10.1186/1471-2180-9-259
5. Muletz Wolz CR, Yarwood SA, Campbell Grant EH, Fleischer RC, Lips KR. Effects of host species and environment on the skin microbiome of Plethodontid salamanders. *Journal of Animal Ecology*. 2018;87(2):341-353. doi:10.1111/1365-2656.12726
6. Turnbaugh PJ, Gordon JI. The core gut microbiome, energy balance and obesity. *Journal of Physiology*. 2009;587(17):4153-4158. doi:10.1113/jphysiol.2009.174136
7. Pershina E V., Ivanova EA, Korvigo IO, et al. Investigation of the core microbiome in main soil types from the East European plain. *Science of the Total Environment*. 2018;631-632:1421-1430. doi:10.1016/j.scitotenv.2018.03.136
8. Salzman S, Whitaker M, Pierce NE. Cycad-feeding insects share a core gut microbiome. *Biological Journal of the Linnean Society*. 2018;123:728-738. https://academic.oup.com/biolinnean/article/123/4/728/4920834
9. Henderson G, Cox F, Ganesh S, et al. Rumen microbial community composition varies with diet and host, but a core microbiome is found across a wide geographical range. *Sci Rep*. 2015;5:1-15. doi:10.1038/srep14567

842 10. Hamady M, Knight R. Microbial community profiling for human microbiome projects:
843 Tools, techniques, and challenges. *Genome Res*. 2009;19(7):1141-1152.
844 doi:10.1101/gr.085464.108
845 11. Hernandez-Teran A, Navarro-Diaz M, Benitez M, Lira R, Wegier A, Escalante AE. Host
846 genotype explains rhizospheric microbial community composition: The case of wild
847 cotton metapopulations (Gossypium hirsutum L.) in Mexico. *FEMS Microbiol Ecol*.
848 2020;96(8):1-11. doi:10.1093/femsec/fiaa109
849 12. Fan K, Chu H, Eldridge DJ, et al. Soil biodiversity supports the delivery of multiple
850 ecosystem functions in urban greenspaces. *Nat Ecol Evol*. 2023;7:113-126.
851 13. Sun L, Li G, Zhao J, Zhang T, Liu J, Zhang J. Core microbiota drive multi-functionality of
852 the soil microbiome in the Cinnamomum camphora coppice planting. *BMC Microbiol*.
853 2024;24(1). doi:10.1186/s12866-023-03170-8
854 14. Björk JR, O'hara RB, Ribes M, Coma R, Montoya JM. The dynamic core microbiome:
855 structure, stability and resistance. *bioRxiv*. Published online 2017:1-50.
856 doi:10.1101/137885
857 15. De Filippis F, La Storia A, Stellato G, Gatti M, Ercolini D. A selected core microbiome
858 drives the early stages of three popular Italian cheese manufactures. *PLoS One*.
859 2014;9(2):1-8. doi:10.1371/journal.pone.0089680
860 16. Risely A. Applying the core microbiome to understand host–microbe systems. *Journal of*
861 *Animal Ecology*. 2020;89(7):1549-1558. doi:10.1111/1365-2656.13229
862 17. Zaura E, Keijser BJ, Huse SM, Crielaard W. Defining the healthy "core microbiome" of
863 oral microbial communities. *BMC Microbiol*. 2009;9(259):1-12. doi:10.1186/1471-2180-
864 9-259
865 18. Ganz HH, Jospin G, Rojas CA, et al. The Kitty Microbiome Project: Defining the Healthy
866 Fecal "Core Microbiome" in Pet Domestic Cats. *Vet Sci*. 2022;9(635):1-21.
867 doi:10.3390/vetsci9110635
868 19. Holyoak GR, Premathilake HU, Lyman CC, et al. The healthy equine uterus harbors a
869 distinct core microbiome plus a rich and diverse microbiome that varies with geographical
870 location. *Sci Rep*. 2022;12(14790):1-14. doi:10.1038/s41598-022-18971-6
871 20. Shade A, Stopnisek N. Abundance-occupancy distributions to prioritize plant core
872 microbiome membership. *Curr Opin Microbiol*. 2019;49:50-58.
873 doi:10.1016/j.mib.2019.09.008
874 21. Shade A, Handelsman J. Beyond the Venn diagram: The hunt for a core microbiome.
875 *Environ Microbiol*. 2012;14(1):4-12. doi:10.1111/j.1462-2920.2011.02585.x
876 22. Camper BT, Kanes AS, Laughlin ZT, Manuel RT, Bewick SA. Transgressive Hybrids as
877 Hopeful Holobionts. *bioRxiv*. Published online 2024:1-68.
878 doi:10.1101/2024.08.17.607925
879 23. Astudillo-García C, Bell JJ, Webster NS, et al. Evaluating the core microbiota in complex
880 communities: A systematic investigation. *Environ Microbiol*. 2017;19(4):1450-1462.
881 doi:10.1111/1462-2920.13647

24. Martiny JBH, Jones SE, Lennon JT, Martiny AC. Microbiomes in light of traits: A phylogenetic perspective. *Science (1979)*. 2015;350(6261):1-8. doi:10.1126/science.aac9323
25. Martiny AC, Treseder K, Pusch G. Phylogenetic conservatism of functional traits in microorganisms. *ISME Journal*. 2013;7(4):830-838. doi:10.1038/ismej.2012.160
26. Callahan BJ, McMurdie PJ, Holmes SP. Exact sequence variants should replace operational taxonomic units in marker-gene data analysis. *ISME Journal*. 2017;11(12):2639-2643. doi:10.1038/ismej.2017.119
27. Větrovský T, Baldrian P. The Variability of the 16S rRNA Gene in Bacterial Genomes and Its Consequences for Bacterial Community Analyses. *PLoS One*. 2013;8(2):1-10. doi:10.1371/journal.pone.0057923
28. Coenye T, Vandamme P. Intragenomic heterogeneity between multiple 16S ribosomal RNA operons in sequenced bacterial genomes. *FEMS Microbiol Lett*. 2003;228(1):45-49. doi:10.1016/S0378-1097(03)00717-1
29. Schloss PD. Amplicon Sequence Variants Artificially Split Bacterial Genomes into Separate Clusters. *mSphere*. 2021;6(4):1-6. doi:10.1128/msphere.00191-21
30. Faith DP. Conservation evaluation and phylogenetic diversity. *Biol Conserv*. 1992;61:1-10.
31. Rao CR. Diversity and Dissimilarity Coefficients: A Unified Approach. *Theor Popul Biol*. 1982;21:24-43.
32. Allen B, Kon M, Bar-Yam Y. A new phylogenetic diversity measure generalizing the shannon index and its application to phyllostomid bats. *American Naturalist*. 2009;174(2):236-243. doi:10.1086/600101
33. Lozupone C, Knight R. UniFrac: A new phylogenetic method for comparing microbial communities. *Appl Environ Microbiol*. 2005;71(12):8228-8235. doi:10.1128/AEM.71.12.8228-8235.2005
34. Tucker CM, Davies TJ, Cadotte MW, Pearse WD. On the relationship between phylogenetic diversity and trait diversity. *Ecology*. 2018;99(6):1473-1479. doi:10.1002/ecy.2349
35. Winter M, Devictor V, Schweiger O. Phylogenetic diversity and nature conservation: Where are we? *Trends Ecol Evol*. 2013;28(4):199-204. doi:10.1016/j.tree.2012.10.015
36. Mouquet N, Devictor V, Meynard CN, et al. Ecophylogenetics: Advances and perspectives. *Biological Reviews*. 2012;87(4):769-785. doi:10.1111/j.1469-185X.2012.00224.x
37. Lankau R, Jørgensen PS, Harris DJ, Sih A. Incorporating evolutionary principles into environmental management and policy. *Evol Appl*. 2011;4(2):315-325. doi:10.1111/j.1752-4571.2010.00171.x
38. Lavergne S, Mouquet N, Thuiller W, Ronce O. Biodiversity and climate change: Integrating evolutionary and ecological responses of species and communities. *Annu Rev Ecol Evol Syst*. 2010;41:321-350. doi:10.1146/annurev-ecolsys-102209-144628

39. Lozupone C, Hamady M, Knight R. UniFrac - An online tool for comparing microbial community diversity in a phylogenetic context. *BMC Bioinformatics*. 2006;7. doi:10.1186/1471-2105-7-371
40. Aguirre De Cárcer D. A conceptual framework for the phylogenetically constrained assembly of microbial communities. *Microbiome*. 2019;7(1):1-11. doi:10.1186/s40168-019-0754-y
41. Talavera-Marcos S, Parras-Moltó M, Aguirre de Cárcer D. Leveraging phylogenetic signal to unravel microbiome function and assembly rules. *Comput Struct Biotechnol J*. 2023;21:5165-5173. doi:10.1016/j.csbj.2023.10.039
42. Parras-Moltó M, Aguirre de Cárcer D. Assessment of phylo-functional coherence along the bacterial phylogeny and taxonomy. *Sci Rep*. 2021;11(1):1-6. doi:10.1038/s41598-021-87909-1
43. Aguirre de Cárcer D. The human gut pan-microbiome presents a compositional core formed by discrete phylogenetic units. *Sci Rep*. 2018;8(1):1-8. doi:10.1038/s41598-018-32221-8
44. Estaki M, Jiang L, Bokulich NA, et al. QIIME 2 Enables Comprehensive End-to-End Analysis of Diverse Microbiome Data and Comparative Studies with Publicly Available Data. *Curr Protoc Bioinformatics*. 2020;70(1):1-46. doi:10.1002/cpbi.100
45. Jaccard P. Distribution de la flore alpine dans le bassin des Dranses et dans quelques régions voisines. *Bulletin de la Société vaudoise des sciences naturelles*. 1901;37:241-272.
46. Lozupone C, Lladser ME, Knights D, Stombaugh J, Knight R. UniFrac: An effective distance metric for microbial community comparison. *ISME Journal*. 2011;5(2):169-172. doi:10.1038/ismej.2010.133
47. Joglekar P, Conlan S, Lee-Lin SQ, et al. Integrated genomic and functional analyses of human skin–associated Staphylococcus reveal extensive inter- and intra-species diversity. *Proc Natl Acad Sci U S A*. 2023;120(47):1-12. doi:10.1073/pnas.2310585120
48. Yang JJ, Chang TW, Jiang Y, et al. Commensal staphylococcus aureus provokes immunity to protect against skin infection of methicillin-resistant staphylococcus aureus. *Int J Mol Sci*. 2018;19(5):1-14. doi:10.3390/ijms19051290
49. Parlet CP, Brown MM, Horswill AR. Commensal Staphylococci Influence Staphylococcus aureus Skin Colonization and Disease. *Trends Microbiol*. 2019;27(6):497-507. https://www.sciencedirect.com/science/article/pii/S0966842X19300216
50. McMurdie PJ, Holmes S. phyloseq: An R package for reproducible interactive analysis and graphics of microbiome census data. *PLoS One*. 2013;8(4).
51. Dubois A. Phylogeny, taxonomy and nomenclature: The problem of taxonomic categories and of nomenclatural ranks. *Zootaxa*. 2007;(1519):27-68. doi:10.11646/zootaxa.1519.1.3
52. Zhou W, Spoto M, Hardy R, et al. Host-Specific Evolutionary and Transmission Dynamics Shape the Functional Diversification of Staphylococcus epidermidis in Human Skin. *Cell*. 2020;180(3):454-470. doi:10.1016/j.cell.2020.01.006

53. Both A, Huang J, Qi M, et al. Distinct clonal lineages and within-host diversification shape invasive staphylococcus epidermidis populations. *PLoS Pathog*. 2021;17(2):1-39. doi:10.1371/JOURNAL.PPAT.1009304
54. Conwill A, Kuan AC, Damerla R, et al. Anatomy promotes neutral coexistence of strains in the human skin microbiome. *Cell Host Microbe*. 2022;30(2):171-182. doi:10.1016/j.chom.2021.12.007
55. Lloyd-Price J, Mahurkar A, Rahnavard G, et al. Strains, functions and dynamics in the expanded Human Microbiome Project. *Nature*. 2017;550(7674):61-66. doi:10.1038/nature23889
56. Murdock SA, Tunnicliffe V, Boschen-Rose RE, Juniper SK. Emergent "core communities" of microbes, meiofauna and macrofauna at hydrothermal vents. *ISME Communications*. 2021;1(27):1-13. doi:10.1038/s43705-021-00031-1
57. García-Machado E, Laporte M, Normandeau E, et al. Fish community shifts along a strong fluvial environmental gradient revealed by eDNA metabarcoding. *Environmental DNA*. 2022;4(1):117-134. doi:10.1002/edn3.221
58. Gelis ERE, Kamal MM, Subhan B, Bachtiar I, Sani LMI, Madduppa H. Environmental biomonitoring of reef fish community structure with eDNA metabarcoding in the Coral Triangle. *Environ Biol Fishes*. 2021;104(8):887-903. doi:10.1007/s10641-021-01118-3
59. Chaumeil PA, Mussig AJ, Hugenholtz P, Parks DH. GTDB-Tk v2: memory friendly classification with the genome taxonomy database. *Bioinformatics*. 2022;38(23):5315-5316. doi:10.1093/bioinformatics/btac672
60. Chaumeil PA, Mussig AJ, Hugenholtz P, Parks DH. GTDB-Tk: A toolkit to classify genomes with the genome taxonomy database. *Bioinformatics*. 2020;36(6):1925-1927. doi:10.1093/bioinformatics/btz848
61. Cavender-Bares J, Kozak KH, Fine PVA, Kembel SW. The merging of community ecology and phylogenetic biology. *Ecol Lett*. 2009;12(7):693-715. doi:10.1111/j.1461-0248.2009.01314.x
62. Graham CH, Storch D, Machac A. Phylogenetic scale in ecology and evolution. *Global Ecology and Biogeography*. 2018;27(2):175-187. doi:10.1111/geb.12686
63. Wanntorp HE, Brooks DR, Nilsson T, et al. Phylogenetic approaches in ecology. *Oikos*. 1990;57(1):119-132. https://www.jstor.org/stable/3565745
64. Mouquet N, Devictor V, Meynard CN, et al. Ecophylogenetics: Advances and perspectives. *Biological Reviews*. 2012;87(4):769-785. doi:10.1111/j.1469-185X.2012.00224.x
65. Hernández CE, Rodríguez-Serrano E, Avaria-Llautureo J, et al. Using phylogenetic information and the comparative method to evaluate hypotheses in macroecology. *Methods Ecol Evol*. 2013;4(5):401-415. doi:10.1111/2041-210X.12033
66. Camper BT, Laughlin ZT, Kanes AS, Manuel RT. A portable and wind resistant drift fence array for arid environments. *bioRxiv*. Published online 2023:1-25. doi:10.1101/2023.09.28.560034

67. Barley AJ, Reeder TW, Nieto-Montes De Oca A, Cole CJ, Thomson RC. A New Diploid Parthenogenetic Whiptail Lizard from Sonora, Mexico, Is the "Missing Link" in the Evolutionary Transition to Polyploidy. *Am Nat*. 2021;198(2):295-309. doi:10.5061/dryad.2z34tmpm2
68. Tucker DB, Colli GR, Giugliano LG, et al. Methodological congruence in phylogenomic analyses with morphological support for teiid lizards (Sauria: Teiidae). *Mol Phylogenet Evol*. 2016;103:75-84.
69. Walker JM, Sullivan BK, Cordes JE. Sanctioned Nomenclature for Triploid Parthenogenetic Colorado Checkered Whiptail and for Other Taxa of the Lizard Genus Aspidoscelis (Family Teiidae). *Herpetol Rev*. 2021;52(3):550-558.
70. Hultman J, Waldrop MP, Mackelprang R, et al. Multi-omics of permafrost, active layer and thermokarst bog soil microbiomes. *Nature*. 2015;521(7551):208-212. doi:10.1038/nature14238
71. R Core Team. R: A language and environment for statistical computing. Published online 2021.

Electronic Supplementary Material

core_community_phylogeny_example.docx

Additional file 1: A simplified system demonstrating the construction of core community phylogenies and calculations of associated metrics.

biom_files.zip

Additional file 2: BIOM files, read counts, taxonomy assignments, microbial phylogenies, and lizard metadata for gut and skin samples used in this study.